View metadata, citation and similar papers at core.ac.uk

brought to you by CORE

provided by Carolina Digital Repository

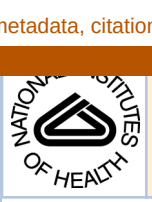

NIH Public Access

Author Manuscript

J Am Chem Soc. Author manuscript; available in PMC 2012 July 27.

Published in final edited form as:

J Am Chem Soc. 2011 July 27; 133(29): 11320–11330. doi:10.1021/ja2034156.

Identification of a Lacosamide Binding Protein Using an Affinity Bait and Chemical Reporter Strategy: 14-3-3 ζ

Ki Duk Park[1], **Dong Wook Kim**[1], **Onrapak Reamtong**[2], **Claire Eyers**[2], **Simon J. Gaskell**[2,3], **Rihe Liu**[1,4,*], and **Harold Kohn**[1,5,*]

[1]Division of Medicinal Chemistry and Natural Products, UNC Eshelman School of Pharmacy, University of North Carolina, Chapel Hill, North Carolina 27599-7568, USA

[2]Michael Barber Centre for Mass Spectrometry, Manchester Interdisciplinary Biocentre, University of Manchester, 131 Princess Street, Manchester, M1 7DN, UK

[3]Queen Mary University of London, Mile End Road, London E1 4NS, UK

[4]Carolina Center for Genome Sciences, University of North Carolina, Chapel Hill, North Carolina 27599-7264, USA

[5]Department of Chemistry, University of North Carolina, Chapel Hill, North Carolina 27599-3290, USA

Abstract

We have advanced a useful strategy to elucidate binding partners of ligands (drugs) with modest binding affinity. Key to this strategy is attaching to the ligand an affinity bait (AB) and a chemical reporter (CR) group, where the AB irreversibly attaches the ligand to the receptor upon binding and the CR group is employed for receptor detection and isolation. We have tested this AB&CR strategy using lacosamide ((*R*)-**1**), a low-molecular-weight antiepileptic drug. We demonstrate that using a (*R*)-lacosamide AB&CR agent ((*R*)-**2**) 14-3-3 ζ in rodent brain soluble lysates is preferentially adducted, adduction is stereospecific with respect to the AB&CR agent, and adduction depends upon the presence of endogenous levels of the small molecule metabolite xanthine. Substitution of lacosamide AB agent ((*R*)- **5**) for (*R*)-**2** led to the identification of the 14-3-3 ζ adduction site (K120) by mass spectrometry. Competition experiments using increasing amounts of (*R*)-**1** in the presence of (*R*)-**2** demonstrated that (*R*)-**1** binds at or near the (*R*)-**2** modification site on 14-3-3 ζ. Structure-activity studies of xanthine derivatives provided information concerning the likely binding interaction between this metabolite and recombinant 14-3-3 ζ. Documentation of the 14-3-3 ζ-xanthine interaction was obtained with isothermal calorimetry using xanthine and the xanthine analogue 1,7-dimethylxanthine.

CORRESPONDING AUTHOR: Division of Medicinal Chemistry and Natural Products, UNC Eshelman School of Pharmacy, University of North Carolina, Chapel Hill, North Carolina 27599-7568 and Department of Chemistry, University of North Carolina, Chapel Hill, North Carolina 27599-3290, hkohn@email.unc.edu, Telephone: 919-843-8112, Fax number: 919-966-0204. Division of Medicinal Chemistry and Natural Products, UNC Eshelman School of Pharmacy, University of North Carolina, Chapel Hill, North Carolina 27599-7568 and Carolina Center for Genome Sciences, University of North Carolina, Chapel Hill, North Carolina 27599-7264, rliu@email.unc.edu, Telephone: 919-843-3635, Fax number: 919-966-0204.

SUPPORTING INFORMATION

Additional experimental details and the full citation for ref 20. MS analysis of purified proteins and modification site. Evaluation and purification of small molecule. Preparation of xanthine solution in HEPES buffer. ITC data with xanthine. Additional competition experiment with BSA as a control protein. Competition experiment with R-18. Sequence alignment of 14-3-3 isoforms. This material is available free of charge via the Internet at http://pubs.acs.org.

NIH-PA Author Manuscript

NIH-PA Author Manuscript

NIH-PA Author Manuscript

NIH-PA Author Manuscript

NIH-PA Author Manuscript

NIH-PA Author Manuscript

INTRODUCTION

Identifying drug targets and elucidating their pharmacological pathways provide the basis for understanding drug function. There have been numerous experimental approaches to identifying and validating targets.[1–10] Microarrays (*e.g.*, nucleic acid, protein, cell, tissue) have proved effective in identifying either genes or proteins whose expression profiles are altered upon drug administration or are present in different levels in diseased tissues. While this approach has revealed global pictures of gene and protein expression profiles, it does not determine which protein target interacts directly with the drug. Antisense technologies, especially RNA interference (RNA_i), provide alternative strategies to identifying and validating drug targets. By knocking down or silencing genes of interest, these technologies mimic the activity of a drug that partially or completely inhibits the normal function of the genes' products. Unfortunately, RNA_i does not directly identify the protein that interacts with the drug of interest. Recently, chemical biology approaches to identifying drug targets have attracted considerable attention. Specifically, forward chemical genetics has been used to identify protein targets and pathways that are chemically modulated.[3–5] Typically, this is accomplished by determining the molecular mechanism(s) that underlie the phenotypic changes induced by small molecules (drugs, drug candidates). Nonetheless, identifying proteins that interact with small molecule therapeutic agents remains a major challenge. This challenge increases for therapeutic agents whose binding to the target is modest. Further complicating target identification studies is the sheer number of binding proteins that could interact with a therapeutic agent, some of which have functional significance but others do not. This is particularly true for neurological agents, such as antiepileptic drugs (AEDs), wherein drug function is often associated with multiple receptor interactions[11,12] and the efficacy of the drug might be the sum of several beneficial interactions.[13,14]

We[15,16] and others[17–26] have advanced a useful strategy to identify binding partners for ligands (low-molecular- weight drugs) that have modest binding affinities for their complementary targets. This approach calls for constructing drug analogues that contain affinity bait (AB) and chemical reporter (CR) units. Upon receptor binding of the drug's AB&CR analogue, covalent attachment of the analogue occurs at the AB site, leading to irreversible, covalent modification of the receptor. Target detection (e.g., in-gel fluorescence) and isolation (e.g., affinity-based chromatographic methods) is accomplished through the CR moiety upon reaction with a bio-orthogonal probe[27,28] and then the isolated bound receptors are identified by mass spectrometry (MS) or other methods.

Our laboratory discovered lacosamide ((*R*)-*N*-benzyl 2-acetamido-3-methoxypropionamide, (*R*)-**1**),[29] a first-in-class AED that has been introduced in the United States and Europe for the adjunctive treatment of partial-onset seizures in adults (Figure 1).[30] The mode of action of (*R*)-**1** is unclear, and only recently has information been presented that this novel drug might modulate sodium channel function.[31,32] We, from our proteomic search for (*R*)-**1**-binding proteins, and others have implicated collapsin-response mediator protein 2 (CRMP2)[15,33,34] and carbonic anhydrase[35] to interact with (*R*)-**1**, but the functional significance of these targets has not been determined.

In this study, we report that 14-3-3 ζ selectively interacts with a lacosamide AB&CR agent and that adduction is specific with respect to the lacosamide AB&CR agent. Significantly, we demonstrate that capture of the target protein is uniquely dependent upon the presence of xanthine, an endogenous small molecule metabolite, in the brain lysate. We show that lacosamide AB&CR adduction of 14-3-3 is isoform specific, and we report the xanthine structural requirements necessary for the lacosamide AB&CR adduction process. Finally, our findings suggest that xanthine is an endogenous modulator of 14-3-3 ζ, a key regulatory protein in the brain. This study validates the AB&CR strategy to identify ligand (drug)

NIH-PA Author Manuscript

NIH-PA Author Manuscript

NIH-PA Author Manuscript

protein binding partners and the need to carefully utilize lysates that closely mimic in vivo conditions in proteomic searches of drug binding targets.

RESULTS

Identification of 14-3-3 ζ as an (*R*)-1 Binding Partner

We chose to use lacosamide AB&CR agent **2**,[15] which contained an isothiocyanate AB group positioned at the 4′-position of the *N*-benzylamide ring and a propargyl CR group located at the C(3) oxy site (Figure 1a). The isothiocyanate group is an established AB moiety[36] that displays an excellent balance between stability and reactivity, while the alkyne moiety in the 3-oxypropargyl residue readily undergoes Cu(I)-mediated cycloaddition reactions[37,38] with azide probes. Accordingly, we used the rhodamine-containing azide probe **3**[15,39] for the in-gel experiments and the biotin-containing azide probe **4**[15] for receptor isolation (Figure 1b). For AB&CR **2** we tested individually both the (*R*)- and (*S*)-enantiomers since the anticonvulsant activity of **1** is associated with the (*R*)-stereoisomer.[29] In the mice maximal electroshock (MES) seizure model,[40] (*R*)-**1** was >22-fold more potent than (*S*)-**1**.[29] Thus, preferential receptor adduction by (*R*)-**2** compared with (*S*)-**2** is an important measure of target site specificity,[41] and it provided a powerful tool to identify binding partners that selectively interact with (*R*)-**1**. We have reported the whole animal pharmacological activities of (*R*)-**2** and (*S*)-**2** in the MES test in both mice (ip) and rats (po).[15] We observed that (*R*)-**2** displayed potent seizure protection while (*S*)-**2** did not but that (*R*)-**2** was approximately 10-fold less active than (*R*)-**1** in mice (ip). More recently, using patch-clamp electrophysiology we determined the functional activity of these compounds in mouse CAD cells.[42] Like (*R*)-**1**,[31] (*R*)-**2** promoted sodium channel slow inactivation without affecting fast inactivation, and sodium channel inactivation was stereoselective with (*R*)-**2** being active but (*S*)-**2** not. These results indicate that our placement of the AB (isothiocyanate) and CR (propargyl) moieties in the lacosamide framework did not markedly affect the modified agent's binding to some of its cognate receptor(s).

We began the study by treating the mouse brain soluble lysate with either (*R*)-**2** or (*S*)-**2** and then reacting the treated lysates with rhodamine probe **3** under Cu(I)-mediated cycloaddition conditions (Figure 1c). We previously evaluated a similar lysate with these probes and identified the preferential adduction of CRMP2, a potential binding target for (*R*)-**1**[33,34] (Figure 1d, arrow).[15] However, the specificity of CRMP2 captured by (*R*)-**2** versus (*S*)-**2** was modest (1.5–1.8-fold). Significantly, the lysate used in this earlier study had been pre-cleared through a gel-filtration NAP-10 column (G-25 resin) to remove small molecules that might react with (inactivate) the isothiocyanate AB group. When the reaction was repeated using the lysate *not treated* with NAP-10, we observed the preferential adduction of another protein(s) located at ~25 kDa (Figure 1c, asterisk). The level of selective adduction by (*R*)-**2** compared with (*S*)-**2** was ≥5:1, significantly greater than that observed for CRMP2. Overall, the level of total protein modification was higher with the NAP-10–treated lysate (Figure 1d) than with the untreated lysate (Figure 1c), a finding consistent with the notion that the NAP-10 column removed lowmolecular- weight nucleophilic molecules (e.g., glutathione) that could react with isothiocyanate containing **2**. Interestingly, we did not observe specific adduction of the ~25 kDa-band in the Nap-10- treated lysate by (*R*)-**2** compared with (*S*)-**2** (Figure 1d), and the level of adduction of the ~25 kDa-band versus other bands in the gel increased when the Nap-10 step was omitted (Figure 1c). To determine the identity of this protein, the experiment was repeated using probe **4** in place of **3** and then the biotinylated products were captured by streptavidin, released by heating in aqueous 1% SDS, and separated using gel chromatography. The ~25-kDa band was excised and analyzed by mass spectrometry (MS) (see Supporting Information Table 1). Two proteins were identified corresponding to 14-3-3 γ and ζ.

NIH-PA Author Manuscript

NIH-PA Author Manuscript

NIH-PA Author Manuscript

To determine if (*R*)-**2** selectively adducted 14-3-3 γ or ζ, the lysate mixture was sequentially treated with either (*R*)-**2** or (*S*)-**2**, rhodamine probe **3**, and immunoprecipitated with antibodies against either 14- 3-3 γ or ζ (Figure 2a). Comparison of the western blots data with those obtained by in-gel fluorescence established that (*R*)-**2** selectively adducted 14-3-3 ζ. To further confirm this finding, we overexpressed C-terminal His-tagged 14-3-3 ζ and added purified recombinant protein to the original lysate for the adduction (Figure 2b). Including the C-terminal His-tag appeared to decrease the electrophoretic mobility of 14-3-3 ζ, thus allowing us to distinguish the recombinant protein from endogenous 14-3-3 ζ. Treatment of the doped lysate samples with either (*R*)-**2** or (*S*)-**2** showed that (*R*)-**2** selectively modified both endogenous and recombinant 14-3-3 ζ to similar extents, which approached ≥5:1.

Knowing that 14-3-3 ζ was selectively modified by (*R*)-**2**, we identified the site of protein modification. Using 14-3-3 ζ, adduction experiments (10 μM, 22 °C, 1 h) were run with (*R*)-**5**.[43] We reported that (*R*)-**5** exhibited excellent seizure protection in the MES test in rodents that exceeded (*R*)-**2** (mice (ip) MES ED_{50} (mg/kg): (*R*)-**2**, 45; (*R*)-**5**, 24; rat (po) MES ED_{50} (mg/kg): (*R*)-**2**, >30; (*R*)-**5**, 4.2), and like (*R*)-**1** and (*R*)-**2** the activity resided principally in the (*R*)-stereoisomer.[43] Furthermore, (*R*)-**5** was >8-fold more potent than (*S*)-**5** in promoting CAD cell sodium channel slow inactivation.[42] MS analysis of the (*R*)-**5** adduction product showed only the presence of a monoadduct and a site where one methionine residue had undergone oxidation (see Supporting Information Figure 1a). The level of monoadduction was modest (~20%). MS-MS of the tryptic digest identified the principal site of adduction as K120, a residue that is conserved in different 14-3-3 isoforms (see Supporting Information Figure 1b). To examine whether K120 is indeed the adduction site, we generated K120A and K120E mutants of His-tagged 14-3-3 ζ by site-directed mutagenesis. In agreement with the MS results, treatment of His-tagged wild-type, K120A, and K120E 14-3-3 ζ proteins with either (*R*)-**2** or (*S*)-**2** showed significantly reduced levels of adduction by (*R*)-**2** for the K120 mutated proteins (Figure 3a). Nonetheless, we observed preferential adduction by (*R*)-**2** compared with (*S*)-**2** for the K120A and K120E 14-3-3 ζ mutants, suggesting that an alternative nucleophilic residue near the binding site of (*R*)- **2** may have been modified when the nucleophilic lysine at position 120 was mutated.

X-ray crystallographic structures of 14-3-3 ζ have been reported.[44–47] Significantly, the K120 residue is not as exposed to solvent as many other lysine residues on the surface of 14-3-3 ζ, suggesting that labeling by the lacosamide AB group in (*R*)-**2** and (*R*)-**5** relies on a binding pocket. The K120 residue is adjacent to a key protein binding pocket in 14-3-3 ζ (Figure 3b),[45] raising the possibility that (*R*)-**1** binding may stabilize a key structural element in the protein or modulate the interaction of 14-3-3 ζ with its binding partners.

Selective Modification of 14-3-3 ζ by (*R*)-2 requires an Endogenous Small Molecule Factor

The loss of selective modification of 14-3-3 ζ by (*R*)-**2** upon lysate treatment with a gel-filtration NAP-10 column (Figure 1d) suggested that either a low-molecular-weight molecule or ion was necessary for efficient and selective labeling of this protein. We observed a similar loss of adduction when the mouse brain lysate was dialyzed with 50 mM HEPES buffer (pH 7.6) using a membrane with 3.5-kDa molecular weight cut-off (data not shown). We suspected the use of a buffer containing this small molecule factor should recover the adduction. Accordingly, the mouse brain soluble lysate was passed through a Centricon 3K membrane filter and the filtrate collected (see Supporting Information Figure 2). We have termed this filtrate, natural buffer. To determine if the endogenous factor remained in the natural buffer, we added recombinant 14-3-3 ζ and bovine serum albumin (BSA), as a control protein, then sequentially treated the reaction sample with either (*R*)-**2** or (*S*)-**2** and rhodamine probe **3** (Figure 4). Parallel experiments were conducted with the untreated mouse brain lysate and with 50 mM HEPES buffer. We observed selective

NIH-PA Author Manuscript

NIH-PA Author Manuscript

NIH-PA Author Manuscript

modification of recombinant 14-3-3 ζ in the untreated lysate and the natural buffer, but not in the 50 mM HEPES buffer, and that the level of (*R*)-**2** specific adduction was ≥5:1. Coomassie blue staining of the gels indicated that the level of proteins present in the natural buffer is low (Figure 4). These findings suggested that the endogenous factor was sufficiently small so as to pass through the Centricon 3K filter.

Key to our identification of the endogenous factor within the soluble lysate was finding that (*R*)-**2** selectively modified 14-3-3 ζ, compared with (*S*)-**2** (≥5-fold), and that (*R*)-**2** preferentially modified recombinant 14-3-3 ζ, compared with BSA control, even though the amount of BSA included in the reaction mixture was greater than His-tagged 14-3-3 ζ (Figure 4). These two diagnostic signatures served as the basis of our bioassay used to identify the endogenous factor.

Prior to isolating the endogenous factor, we boiled the natural buffer from mouse brain lysate to determine if the factor underwent heat denaturation. Similarly, we treated the natural buffer with divalent chelating agents (EDTA (2 mM), EGTA (1 mM)) to determine if metals, such as Mg^{2+} and Zn^{2+}, were the endogenous factor (see Supporting Information Figure 3). Using our bioassay, both treatments provided high (*R*)-**2** versus (*S*)-**2** adduction selectivity, suggesting that the endogenous factor was neither a small protein nor a divalent metal ion. Moreover, the endogenous factor appeared sufficiently stable to survive most isolation procedures.

The endogenous factor isolation protocol is provided in the Supporting Information Figure 2. We chose to use rat rather than mouse brain soluble lysates to provide larger lysate samples. (*R*)-**1**[29] showed comparable levels of seizure protection in the mouse and rat. Prior to isolating the endogenous factor, we compared the gel patterns obtained from both untreated rodent brain lysates after sequential reaction with either (*R*)-**2** or (*S*)-**2**, followed by rhodamine probe **3** treatment (see Supporting Information Figure 4). As expected, we observed selective adduction of 14-3-3 ζ by (*R*)-**2** compared with (*S*)-**2** in both soluble lysates, thereby insuring the presence of the endogenous factor in the rat brain lysate. Accordingly, the rat brain natural buffer lysate was first sequentially extracted with ethyl acetate, methylene chloride, and hexanes to remove lipophilic constituents. The aqueous layer was separated on a Sephadex G-25 column (see Supporting Information Figure 5a) and then a reverse-phase C-18 column (see Supporting Information Figure 5b). At every stage, fractions were tested using the in-gel, fluorescence-based bioassay wherein recombinant 14-3-3 ζ and BSA were added to the fractions and then evaluated with (*R*)-**2** and (*S*)-**2** (data not shown). ^{1}H NMR spectroscopy was instrumental in our identification of the endogenous factor. We obtained ^{1}H NMR spectra for the active fractions and the surrounding fractions that were partially active or inactive. Comparative analysis allowed us to tentatively identify compounds of interest as well as other biomolecules in the active fractions. Supporting Information Figure 6a and 6b show the ^{1}H NMR spectra of two different active fractions obtained from different isolation efforts after the C-18 column (the fractions were obtained using different eluant water/methanol compositions). Two sets of peaks were common to both spectra (indicated by red and black arrows), which we have tentatively identified as glycerol and xanthine (**6**) (see Supporting Information Figure 6). Using this information, we tested to see if either of these biomolecules (0.5 mM) would lead to selective (*R*)-**2** versus (*S*)-**2** adduction when added to a 50 mM HEPES buffer solution containing His-tagged 14-3-3 ζ and BSA. We also tested a range of other biomolecules that may have been present in the active fractions, including ATP, ADP, AMP, cAMP, GTP, GMP, ITP, adenosine, guanosine, inosine, adenine, guanine, hypoxanthine, phenylalanine, serine, and GABA. Only xanthine led to the selective modification of recombinant 14-3-3 ζ by (*R*)-**2** compared with (*S*)-**2**, and the selective (*R*)-**2** adduction of 14-3-3 ζ versus BSA (data not shown). We also monitored the relative amounts of xanthine in the active C-18 fractions by HR-MS (see

NIH-PA Author Manuscript

NIH-PA Author Manuscript

NIH-PA Author Manuscript

Supporting Information Figure 7). The HR-MS confirmed the presence of xanthine in the active fractions and documented that the relative abundance of xanthine in these fractions mirrored the observed selectivity of (*R*)-**2** versus (*S*)-**2** adduction in the in-gel experiments (see Supporting Information Figure 5b).

We determined a dose dependency for xanthine modulation of (*R*)-**2** adduction of His-tagged 14-3-3 ζ in 50 mM HEPES solutions (Figure 5a). Preferential (*R*)-**2** versus (*S*)-**2** 14-3-3 ζ modification was observed at xanthine concentrations as low as 31.3 μM and steadily increased as the xanthine concentration was raised to 250 μM. At 62.5 μM xanthine, we estimated the selectivity was ~2:1. Furthermore, we observed little difference in the extent of xanthine-mediated (*R*)-**2** selective protein modification in either the absence or the presence of Mg^{2+} ions (2 mM) and further showed that 14-3-3 ζ was preferentially modified compared with BSA (Figure 5b).

(*R*)-2 Modification of 14-3-3 is Isoform Specific

14-3-3 proteins are a family of conserved regulatory molecules expressed in all eukaryotic cells.[48] They consist of seven homologous isoforms that are presumed to have some redundant biological functions. We determined whether or not (*R*)-**2** modification was selective to a specific 14-3-3 isoform using our bioassay in the natural buffer (Figure 6a). Significantly, when we used commercial samples of all seven non-phosphorylated 14-3-3 isoforms, only 14-3-3 ζ was selectively adducted by (*R*)-**2**, compared with (*S*)-**2** (Figure 6a), and further the 14-3-3 ζ was preferentially modified compared with BSA (data not shown). This finding documented that (*R*)-**2** modification was highly isoform selective, despite the homologous nature of this family of proteins.

The Xanthine Structure-Activity Relationship for (*R*)-2 Modification of Recombinant 14-3-3 ζ

We determined the structure-activity relationship (SAR) for the exogenous factor, xanthine (**6**). Xanthine is a metabolite derived from the ATP and inosine degradation pathways.[49] It is also a common core structure of an important class of natural products. Thus, we tested three *N*-monomethyl derivatives of xanthine (N-1 (**7**), N-3 (**8**), N-7 (**9**)), three *N*,*N*′-dimethyl derivatives (**10** (theophylline (N-1, N-3)), **11** (N-1, N-7), **12** (theobromine (N-3, N-7))) and one *N*, *N*′, *N*″-trimethyl derivative (**13** (caffeine (N-1, N-3, N-7)), along with uric acid (**14**), a metabolite produced from xanthine (Figure 6b).[49] Of these compounds, only 1-methylxanthine (**7**), 7-methylxanthine (**9**), and 1,7-dimethylxanthine (**11**) exhibited preferential (*R*)-**2** versus (*S*)-**2** modification of recombinant 14-3-3 ζ comparable to that observed for xanthine (Figure 6c). This pattern suggested that xanthine binding with 14-3-3 ζ is facially dependent and that binding likely occurs at the N-3 edge of the purine metabolite.

1,7-Dimethylxanthine Binding to 14-3-3 ζ

We determined if 1,7-dimethylxanthine binds to recombinant 14-3-3 ζ using isothermal calorimetry (ITC). We chose 1,7-dimethylxanthine based on our xanthine SAR studies and the enhanced water solubility of 1,7-dimethylxanthine compared with xanthine. Accordingly, we added a moderately high concentration of 1,7-dimethylxanthine (10 mM) to a solution of recombinant 14-3-3 ζ (200 μM) in phosphate buffer solution (pH 7.6) and obtained a binding isotherm (Figure 7), showing that binding was endothermic. Using Origin 7.0 software, we saw that the binding isotherm for 1,7-dimethylxanthine converged and fit best to a binding site model with a K_d of 68 ± 5.3 μM and a corresponding *c* value of 10.5. Knowing this, we repeated the binding study using a dilute solution of xanthine (1 mM) in place of 1,7-dimethylxanthine and recombinant 14-3-3 ζ (100 μM). Under these

NIH-PA Author Manuscript

NIH-PA Author Manuscript

NIH-PA Author Manuscript

conditions, we obtained an approximate K_d of 29 ± 7.2 μM (c = 3.4) (see Supporting Information Figure 8).

Efforts to detect (*R*)-**1** binding to solutions containing recombinant 14-3-3 ζ in the absence of either xanthine or 1,7-dimethylxanthine were unsuccessful. However, small changes were observed in the ITCs for (*R*)-**1** versus (*S*)-**1** in the presence of 1,7-dimethylxanthine and recombinant 14-3-3 ζ, but we were unable to confidently assign these changes to specific protein binding by (*R*)-**1**.

(*R*)-1 Binds at or near the (*R*)-2 Modification Site on 14-3-3 ζ

To determine if (*R*)-**1** binds near the (*R*)-**2** 14-3-3 ζ modification site, we added increasingly amounts of (*R*)-**1** into the reaction solutions containing high levels of 14-3-3 ζ (20 μg/50 μL reaction volume), the control protein, enolase (30 μg/50 μL reaction volume), and 1,7-dimethylxanthine (0.5 mM) and using a short incubation time (2 min) conditions that was similar to those employed in other competition experiments.[50] In the absence of (*R*)-**1** we observed selective modification of 14-3-3 ζ by (*R*)-**2** compared with (*S*)-**2**, and the preferential modification of 14-3-3 ζ versus the control protein (Figure 8a, b lanes 1 and 2). The relative levels of 14-3-3 ζ-to-enolase modification surpassed that found for 14-3-3 ζ-to-BSA (Figure 8a and Supporting Information Figure 9a). Upon addition of competing amounts of (*R*)-**1** we witnessed a steady decrease in the level of 14-3-3 ζ modification as the number of equivalents of (*R*)-**1** was increased (Figure 8a, lanes 3–5). Repetition of this experiment using (*S*)-**1** in place of (*R*)-**1** led to no noticeable loss in the (*R*)-**2** modification level (Figure 8a, lanes 6–8).

DISCUSSION

Our proteomic AB&CR strategy was designed to identify ligand (drug)-receptor interactions in which binding was modest.[15,17–26] We have outlined the structural requirements for the AB and CR units installed within the lacosamide framework.[15] Key to the strategy is selecting AB and CR units that do not impede binding of the lacosamide AB&CR agent to the (*R*)-**1** binding site(s). The AB group should be sufficiently stable to permit dissolution and protein binding yet sufficiently reactive to irreversibly modify the target. The CR moiety must readily undergo bio-orthogonal coupling with a suitable probe. We prepared both C(2) stereoisomers of the lacosamide AB&CR agent since anticonvulsant activity of the drug resided principally in the (*R*)-isomer (D-configuration).[29] Accordingly, we evaluated both (*R*)-**2** and (*S*)-**2** in the in vivo MES model[37] for differentiation of stereoisomers in activity of this AB&CR agent.[15] We found that (*R*)-**2** was >6.7-fold more active than (*S*)-**2** in mice (ip). Similarly, we found that (*R*)-**5** displayed potent anticonvulsant activity in mice (ip) and rats (po).[43] Nonetheless, we recognized that the promising pharmacological data do not guarantee that these compounds' function is similar to (*R*)-**1** or that they will act as site-selective agents. Recent patch-clamp electrophysiology studies with CAD cells demonstrated that AB&CR (*R*)-**2** and AB (*R*)-**5**, like (*R*)-**1**,[31,32] modulated sodium channel slow inactivation processes and did not affect fast inactivation processes.[42] When (*R*)-**2** was compared with (*S*)-**2**, the IC_{50} for (*R*)-**2** was >10-fold lower (more active) than (*S*)-**2**, a finding in close agreement with the differences in the anticonvulsant activities for these two stereoisomers in the MES test in mice (ip). A similar finding was observed for (*R*)-**5** versus (*S*)-**5**.[42] These collective findings indicate that the AB&CR (*R*)-**2** and the AB (*R*)-**5** agents serve as excellent surrogates for (*R*)-**1**.

Our knowledge of (*R*)-**1** function is evolving. Whole animal pharmacological studies showed that (*R*)- **1** anticonvulsant activity is unique and prevents seizure spread by mechanisms different from those of other AEDs.[29,51] Radioligand displacement assays using more than 100 potential receptors did not reveal any high-affinity binding targets.[33]

NIH-PA Author Manuscript

NIH-PA Author Manuscript

NIH-PA Author Manuscript

This finding suggested that either the target(s) is novel or the binding is weak or both. Recently, patch-clamp electrophysiology experiments have shown that (*R*)-**1** modulated the slow inactivation gate in sodium channels without affecting fast inactivation processes.[31,32] (*R*)-**1** is the only AED known to preferentially affect the sodium channel's slow inactivation. Separate studies have shown that (*R*)-**1** binds to CRMP2[15,33,34] and carbonic anhydrase,[35] but the functional significance of these results remains unclear. Thus, we investigated the untreated rodent brain soluble lysate using our AB&CR strategy to identify other (*R*)-**1**–interacting proteins that may bind the AED.

Using a mouse brain soluble lysate without depleting small molecules, we identified a band at ~25 kDa that was preferentially adducted by AB&CR (*R*)-**2**, compared with (*S*)-**2** (Figure 1c). This selective adduction served as an important measure of target site specificity and paralleled the anticonvulsant activities of (*R*)-**1** and (*S*)-**1**.[29] Furthermore, the ~25 kDa-band was extensively modified compared with other higher molecular weight protein bands. Both the specificity for the (*R*)-enantiomer adduction and the extent of adduction differed from the same lysate in which small molecules have been depleted by passing through a Nap-10 column prior to treatment with the AB&CR agent (Figure 1d). MS confirmed the presence of 14-3-3 proteins (γ, ζ) (Supporting Information Table 1), and we further identified by immunoprecipitation that 14-3-3 ζ was preferentially adducted by (*R*)-**2** (Figure 2a). Adding overexpressed His-tagged 14-3-3 ζ to lysate led to selective adduction of the protein by (*R*)-**2**, compared with (*S*)-**2** (Figure 2b).

The 14-3-3 proteins are a family of conserved regulatory molecules expressed in all eukaryotic cells.[48] The 14-3-3 proteins are abundant in the brain, comprising approximately 1% of its total soluble protein.[52] They consist of seven homologous isoforms, which are presumed to have some redundant biological functions. A characteristic feature of 14-3-3 proteins is their ability to bind to a wide variety of functionally diverse signaling proteins.[52] More than 100 signaling proteins have been reported as 14- 3-3 interacting partners.[53] 14-3-3 proteins are present as either homodimers or heterodimers and contain different domains or regions for divalent cation binding, post-translational modification, and proteolytic cleavage. Crystal structure analysis shows that 14-3-3 proteins have a cup-shaped dimeric structure,[44–46] with each monomer containing nine α-helices organized in an antiparallel manner to form an L-shaped structure. The interior of this structure contains a highly conserved concave amphipathic groove, which is the site where the 14-3-3 protein interacts with its binding motifs that often contain a phosphorylated serine or threonine residue.[47,54] It is notable that K120, the (*R*)-**5** modification site identified by MS (see Supporting Information Figure 1), is adjacent to this amphipathic groove (Figure 3b), suggesting that (*R*)-**1** binding near this locus could affect 14-3-3 ζ interaction with its binding partners. Since K120 is in close proximity to the established binding site for the R-18 protein[45] (Figure 3b), we tested whether R- 18 competitively blocked (*R*)-**2** covalent modification of 14-3-3 ζ (see Supporting Information Figure 10). We observed that inclusion of R-18 (3.5–7 equiv) with recombinant 14-3-3 ζ in natural buffer led to a dose-dependent reduction in (*R*)-**2** adduction levels.

We were surprised to find that preferential modification of 14-3-3 ζ by (*R*)-**2** compared with (*S*)-**2** depended on xanthine's being present in the lysate medium (Figures 4 and 5). When the lysate was either passed through a NAP-10 column (Figure 1d) or dialyzed against HEPES buffer we observed minimal adduction of the ~25-kDa-band associated with 14-3-3 ζ and no difference in the extent of modification by (*R*)-**2** versus (*S*)-**2**. In the presence of xanthine and using only HEPES buffer, the observed selectivity for 14-3-3 ζ was ≥5:1 (Figure 5b), a value far higher than observed for CRMP2 (1.5–1.8-fold; Figure 1d) and one that mirrored the differences in anticonvulsant activities in the whole animal MES seizure model.[29] The effect of xanthine on (*R*)-**2** adduction was dose dependent and could be seen as

NIH-PA Author Manuscript

NIH-PA Author Manuscript

NIH-PA Author Manuscript

low as 31.3 μM (Figure 5a) and irrespective of Mg^{2+} (Figure 5b). Using the in vitro bioassay conditions, we also demonstrated that xanthine enhanced the selective adduction of 14-3-3 ζ compared with BSA control, suggesting that xanthine binding to 14-3-3 ζ facilitated (*R*)-**2** adduction.

We determined the SAR for xanthine-mediated adduction of 14-3-3 ζ by (*R*)-**2**. Using eight methylated xanthine derivatives (Figure 6b), we showed that methylation of the N(3) site in xanthine led to a loss of the facilitating effect (Figure 6c). This finding indicated that this facial side in xanthine derivatives interacts with the 14-3-3 ζ surface, possibly leading to a conformation change that permits (*R*)-**2** adduction.

Evidence to support xanthine interaction with recombinant 14-3-3 ζ was gained using ITC where a binding isotherm was observed for 1,7-dimethylxanthine, providing a K_d value of 68 ± 5.3 μM (Figure 7). The ITC experiment showed that binding was endothermic, which indicated that favorable entropic changes leading to a net increase in disorder accompanied the binding of this xanthine derivative. A comparably endothermic binding isotherm for xanthine was observed and provided a K_d value of 29 ± 4.2 μM (see Supporting Information Figure 8). Similar endothermic binding processes have been observed for other biomolecular interactions. For example, addition of porcine pancreatic trypsin to soybean trypsin inhibitor leads to a favorable interaction with moderate affinity but is endothermic.[55]

Recently, xanthine levels have been determined in both rat[56] and human[57,58] brain tissues using HPLC and a cooled column, and in the human cerebrospinal fluid.[59,60] Xanthine levels in brain tissues were shown to increase with time due to post mortem metabolic degradation of nucleosides in the brain. In the rat brain, the xanthine level 30 sec after surgical removal was 50.53 μmol/kg of wet tissue, which increased to 110.80 μmol/kg and 158.60 μmol/kg after 4 h and 24 h storage at 25 °C, respectively.[56] The corresponding values in the human brain were 26.57 μmol/kg, 42.51 μmol/kg, and 110.78 μmol/kg.[56] By comparisons, reported xanthine concentrations in the cerebrospinal fluid of humans spanned from ~2.6 to 13 μM.[59,60] In our study, we used both intact frozen (−78 °C) mice and rat brain tissues obtained from the supplier and the soluble lysate prepared at room temperature within 4 h and then diluted with buffer (~5-fold) to give a known volume of lysate prior to use. Using the literature rat value[56] (110.80 μmol/kg) for 4 h at 25 °C, we estimated that the xanthine level in our soluble brain lysate after dilution was ~22 μM; such value that may be higher if metabolic degradation in lysate proceeded to a greater extent than in the intact whole brain. The ~22 μM xanthine concentration is close to the measured K_d value for the xanthine-14-3-3 ζ complex (K_d = 29 ± 4.2 μM), suggesting that appreciable amounts of the protein may be bound to xanthine, and thus responsible for the specificity of the (*R*)-**2** adduction process. Nonetheless, we cannot exclude that other, unidentified modulators in the lysate may have facilitated the observed selective (*R*)-**2** adduction process. Moreover, we recognize that the interaction of 14-3-3 ζ with other proteins in the cellular milieu might further enhance the binding of xanthine to 14-3-3 ζ.

We are unaware of xanthine's being reported to be a modulator of 14-3-3 function. In the brain of mammals, adenine triphosphate (ATP) degradation is associated with glutamate-mediated excitotoxicity.[59] ATP is sequentially metabolized providing inosine and then hypoxanthine.[49] Hypoxanthine is metabolized to xanthine by xanthine oxidoreductase. Xanthine is also produced from guanine by guanine deaminase.[49] Since ATP is a metabolic source for purine metabolites, the cerebrospinal fluid levels of xanthine and other metabolites have been determined in patients with different neurological disorders (i.e., epilepsy, stroke, muscular sclerosis, myelopathy, viral meningitis). Interestingly, patients with these conditions showed a 1.7-fold increase over controls in xanthine levels.[59] Accordingly, due to the relative abundance of xanthine in brain tissues it will be important

NIH-PA Author Manuscript

NIH-PA Author Manuscript

NIH-PA Author Manuscript

to determine if this metabolite is involved in modulating the select 14-3-3 ζ regulatory pathways, and if this is controlled, in part, by pathological processes.

Our studies using the mouse brain soluble lysate showed that only 14-3-3 ζ was selectively modified by (*R*)-**2**. Nonetheless, we asked whether the other unphosphorylated 14-3-3 isoforms in the presence of xanthine were selectively modified by (*R*)-**2** compared with (*S*)-**2** (Figure 6a). Of the seven isoforms, selective adduction was detected only for 14-3-3 ζ, indicating that this adduction is highly isoform specific. This finding was surprising in context of the primary sequences surrounding the K120 adduction site for 14-3-3 ζ and the corresponding sequences for the other 14-3-3 isoforms (see Supporting Information Figure 11). We found that the immediate residues surrounding the K120 site in 14-3-3 ζ are highly conserved in the other isoforms, but that sequences out of this motif are diverse. Without the corresponding co-crystallographic data for the 14-3-3 ζ/xanthine complex we are unable to rationalize the observed selectivity (Figure 6a).

Finding that (*R*)-**2** selectively adducted 14-3-3 ζ in the rodent brain soluble lysate led us to determine the binding interaction of the parent agent, (*R*)-**1**, with recombinant 14-3-3 ζ by ITC. We were not able to detect (*R*)-**1** binding to recombinant 14-3-3 ζ in the absence of xanthine. Including 1,7- dimethylxanthine led to a small difference in the isotherms for (*R*)-**1** compared with (*S*)-**1**, but we could not confidently assign these to selective binding of (*R*)-**1** to a 1,7-dimethylxanthine/14-3-3 complex. This was not unexpected, since the analysis of an ITC binding isotherm is difficult for systems with small binding constants.[61] Thus, we documented that (*R*)-**1** binds near the (*R*)-**2** modification site in 14- 3-3 ζ in the presence of 1,7-dimethylxanthine by a competition experiment using excess amounts of (*R*)- **1** to block the (*R*)-**2** adduction process using an established procedure[50] (Figure 8a). We observed that (*R*)-**1**, but not (*S*)-**1**, inhibited adduction in a dose-dependent manner.

The functional significance of (*R*)-**1** binding to 14-3-3 ζ remains unknown. Reports indicate that 14-3- 3 proteins play an essential role in controlling the function and expression of diverse ion channels. In mouse cardiac myocytes, 14-3-3 η interacts with the cytoplasmic I interdomain of $Na_V1.5$, and such interaction induces a negative shift in the inactivation curve of the sodium current while the activation curve and the current density are not changed.[62] In the rat brain, the chloride intracellular channel protein (Clic4) binds directly to 14-3-3 ζ and dynamin I and possibly influences its roles in membrane trafficking.[63] A recent study described direct modulation of $Ca_V2.2$ channel inactivation properties by 14-3-3.[64] Interference with 14-3-3 binding in hippocampal neurons accelerates $Ca_V2.2$ channel inactivation and enhances short-term synaptic depression.[64] Finding 14-3-3 ζ as a putative (*R*)-**1** target raises the possibility that the 14-3-3 ζ-mediated ion channel function might be modulated by the drug. Nonetheless, we recognize that not all binding interactions have physiological consequences. For example, both CRMP2[15,33,34,65] and carbonic anhydrase[35] interact with (*R*)-**1**, but their physiological relevance for drug function remains unclear. Thus, detailed studies are underway to examine the impact of (*R*)-**1** binding to 14-3-3 ζ and whether this interaction can contribute to its pronounced antiepileptic activity.

CONCLUSIONS

An important outcome of this study was validating the AB&CR strategy to identify binding partners of ligands (drugs) that have modest binding.[15,17–26] Using (*R*)-**2** we identified 14-3-3 ζ as a potential lacosamide target. We suggest that most other proteomic methods would not be sensitive enough to identify this interaction, thus demonstrating the power of the AB&CR approach. A second important finding was that the metabolite xanthine binds with14-3-3 ζ. We are not aware of prior studies reporting that xanthine is a 14-3-3 modulator. It will be interesting to determine the role of xanthine on 14-3-3 ζ signaling

NIH-PA Author Manuscript

NIH-PA Author Manuscript

NIH-PA Author Manuscript

pathways and how the levels of xanthine in the central nervous system affect different pharmacological pathways. A third finding was the demonstration that 14-3-3 ζ is a binding partner of (*R*)-**1**. (*R*)-**2** modification was stereospecific and preferentially occurred with 14-3-3 ζ compared with other proteins in the soluble brain lysate or added control proteins (i.e., BSA, enolase). Finally, the observation that xanthine was critical for the (*R*)-**2** modification of 14-3-3 ζ emphasizes the need to utilize in vitro proteomic target search conditions that closely parallel the in vivo setting. Our current understanding of the proteome and its cellular environment is sufficiently incomplete to allow us to anticipate all the required interactions for ligand (drug) binding to a given receptor. Knowing this, it makes sense to employ a test system that only minimally disrupts the proteome environment.

EXPERIMENTAL SECTION

Preparation of Brain Soluble Proteomes

Either mouse brains (male, 2 months, ICR mice, Rockland Immunochemicals) or rat brains (male, 2 months, Sprague Dawley strain, Rockland Immunochemicals) were Dounce-homogenized in 50 mM HEPES buffer (pH 7.6). The lysate was centrifuged at slow speed (1200 × g for 12 min at 4 °C) to remove debris. The supernatant was then centrifuged at high speed (100,000 × g for 1 h at 4 °C). The resulting supernatant was collected and stored at −80 °C until use. The total protein concentration was determined using the Bradford assay.

Probe Labeling, Cycloaddition Reaction, and In-Gel Fluorescence Scanning (Method A)

Brain soluble proteomes (50 μL, 4.0 mg/mL protein in 50 mM HEPES buffer (pH 7.6)) were treated with **2** (10 μM) at room temperature (5–30 min). The modified lysates was sequentially treated with rhodamine reporter tag **3** (rhodamine-azide (Rho-N_3) (50 μM)), TCEP (1 mM), TBTA (100 μM) and $CuSO_4$ (1 mM). Samples were shaken and allowed to rotate using Roto-shake (8 rpm) at room temperature (5–30 min). SDS-PAGE loading buffer (2×) was added to the proteins and then they were separated by SDS-PAGE and visualized by in-gel fluorescence using a typhoon 9400 scanner (Amersham Bioscience), with excitation at 532 nm and detection at 580 nm.

In-Gel Fluorescence Using the Over-Expressed His-tagged 14-3-3 ζ

His-tagged 14-3-3 ζ protein and BSA as internal standard solution (50 μL, 0.2 mg/mL of 14-3-3 ζ protein and 0.4 mg/mL of BSA in 50 mM HEPES buffer (pH 7.6)) were added to either the lysate, natural buffer, or phosphate buffer, then labeled using Method A and visualized by in-gel fluorescence.

Purification of Probe-labeled Proteins

Mouse brain lysate (200 μL of 4.0 mg/mL protein in 50 mM HEPES buffer (pH 7.6)) was treated with (*R*)-**2** (20 μM) at room temperature (30 min). To the modified lysate was sequentially added **4** (100 μM), TCEP (500 μM), TBTA (100 μM) and $CuSO_4$ (1 mM). The samples were shaken and allowed to rotate using Roto-shake (8 rpm) at room temperature (1 h). After passage through a NAP-5 column, the sample was added to an immobilized streptavidin slurry (0.3 mL) (high-capacity streptavidin agarose resin, Pierce) and rotated (15 rpm) at 4 °C (90 min). The streptavidin beads were sequentially washed with aqueous 0.1% Triton X-100/15 mM HEPES buffer (pH 7.4) (3 × 0.8 mL), an aqueous 6 M urea solution (3 × 0.8 mL), and an aqueous 15 mM HEPES buffer (pH 7.4) (4 × 0.8 mL). The beads were centrifuged (1000 rpm, 1 min), and the supernatant removed. The beads were treated with loading buffer (aqueous 1% SDS, 10% glycerol, 1% mercaptoethanol, 0.01%

NIH-PA Author Manuscript

NIH-PA Author Manuscript

NIH-PA Author Manuscript

bromophenol blue (final concentration)) (95 °C, 5 min). The samples were loaded on a 10% SDS-PAGE gel and the proteins were visualized by silver staining.

Immunoprecipitation

Utilizing proteomic Method A, mouse brain lysates (50 μL of 4.0 mg/mL protein in 50 mM HEPES buffer (pH 7.6)) were treated with **2** (10 μM) at room temperature (30 min). The modified proteins (50 μL) were treated with Rho-N_3 (**3**) under Cu(I)-mediated cycloaddition conditions. The aliquots (8 μL) of samples were loaded on 10% SDS-PAGE and visualized by in-gel fluorescence. The remaining samples (42 μL) was treated with either 14-3-3 ζ antibody (2 μg, sc-1019, Santa Cruz Biotechnology) or 14-3-3 γ (2 μg, sc-731, Santa Cruz Biotechnology) and incubated at 4 °C (1 h). The samples were then added to a protein A/G agarose slurry (30 μL) (Protein A/G PLUSAgarose, Santa Cruz Biotechnology) and rotated (15 rpm) at 4 °C (1 h). The beads were washed with aqueous RIPA buffer (3 × 0.2 mL) and aqueous 15 mM HEPES buffer (pH 7.4) (2 ×0.2 mL). The beads were centrifuged (1000 rpm, 1 min), and the supernatant removed. The beads were treated with loading buffer (aqueous 1% SDS, 10% glycerol, 1% mercaptoethanol, 0.01% bromophenol blue [final concentration]) (95 °C, 5 min). The samples were loaded onto two 10% SDS-PAGE gels and the proteins visualized by western blot and in-gel using a typhoon 9400 scanner with excitation at 532 nm and detection at 580 nm.

Preparation of Natural Buffer and Purification of Small Molecule Factor

Rat brains (5 g, male, 2 months, Sprague Dawley strain, Rockland Immunochemicals) were Dounce-homogenized in 50 mM HEPES buffer (25 mL, pH 7.6). The lysate was centrifuged at slow speed (1200 × g for 12 min at 4 °C) to remove debris. The supernatant was then centrifuged at high speed (100,000 × g for 1 h at 4 °C). The resulting supernatant (20 mL) was centrifuged (× 3700 *g*, 1 h) using a Centricon (UFC800324, Millipore) to remove proteins. The resulting solution (natural buffer) was extracted with organic solvents (n-hexanes, EtOAc and CH_2Cl_2, sequentially, (20 mL, × 3 each)). The aqueous layer was concentrated in vacuo. The residue was loaded on a Sephadex G-25 size exclusion column (17-0033-01, GE Healthcare), and water was used as the eluent and 5-mL fractions were collected. The fractions were tested using in-gel fluorescence after addition of His-tagged 14-3-3 ζ (0.3 mg/mL), BSA (0.6 mg/mL), **2** (10 μM), and **3** (Method A) and the active fractions were collected and concentrated in vacuo. The resulting residue containing the active fractions was separated on a C-18 reversed–phase silica gel column (60756, Fluka) using water/MeOH (10:0 ~ 9:1, v/v) as the eluent and then tested for activity after adding His-tagged 14-3-3 ζ (0.3 mg/mL), BSA (0.6 mg/mL), **2** (10 μM), and **3** (Method A). The active fractions were analyzed by ^{1}H NMR and HR-MS.

Competition Experiment

Utilizing proteomic Method A, His-tagged 14-3-3 ζ protein and enolase as internal standard solution (50 μL, 0.4 mg/mL of 14-3-3 ζ protein and 0.6 mg/mL of enolase in 50 mM HEPES buffer (pH 7.6) including 0.5 mM of 1,7-dimethylxanthine) and either excess (*R*)-**1** or (*S*)-**1** were treated with **2** (40 μM) at room temperature (2 min) followed by Cu(I)-mediated cycloaddition with **3** at room temperature (5 min). The proteins were visualized by in-gel fluorescence.

Supplementary Material

Refer to Web version on PubMed Central for supplementary material.

NIH-PA Author Manuscript

NIH-PA Author Manuscript

NIH-PA Author Manuscript

Acknowledgments

We thank the NINDS and the Anticonvulsant Screening Program (ASP) at the National Institutes of Health. This work was supported by the National Institute of Neurological Disorders and Stroke (R01NS054112) and by the Korean Research Foundation Grant (KRF-2006-352-C00042). We thank one of the reviewers of this paper for the reviewer's thoughtful comments that led us to conduct additional studies. Harold Kohn has a royalty-stake position in (*R*)-**1**.

References

1. Wang S, Sim TB, Kim YS, Chang YT. Curr Opin Chem Biol. 2004; 8:371–377. [PubMed: 15288246]
2. Burdine L, Kodadek T. Chem Biol. 2004; 11:593–597. [PubMed: 15157870]
3. Schreiber SL. Nature Chem Biol. 2005; 1:64–66. [PubMed: 16407997]
4. Alaimo P, Shogren-Knaak MA, Shokat KM. Curr Opin Chem Biol. 2001; 5:360–367. [PubMed: 11470597]
5. Meisner NC, Hintersteiner M, Uhl V, Weidemann T, Schmied M, Gstach H, Auer M. Curr Opin Chem Biol. 2004; 8:424–431. [PubMed: 15338571]
6. Doyle DF, Braasch DA, Jackson LK, Weiss HE, Boehm MF, Mangelsdorf DJ, Corey DR. J Am Chem Soc. 2001; 123:11367–11371. [PubMed: 11707111]
7. Suwwan de Felipe K, Carter BT, Althoff EA, Cornish VW. Biochemistry. 2004; 43:10353–10363. [PubMed: 15301533]
8. Hussey SL, Muddana SS, Peterson BR. J Am Chem Soc. 2003; 125:3692–3693. [PubMed: 12656587]
9. SenGupta DJ, Zhang B, Kraemer B, Pochart P, Fields S, Wickens M. Proc Natl Acad Sci USA. 1996; 93:8496–8501. [PubMed: 8710898]
10. Licitra EJ, Liu JO. Proc Natl Acad Sci USA. 1996; 93:12817–12821. [PubMed: 8917502]
11. Roth BL, Sheffler DJ, Kroeze WK. Nat Rev Drug Discov. 2004; 3:353–359. [PubMed: 15060530]
12. Cavalli A, Bolognesi ML, Minarini A, Rosini M, Tumiatti V, Recanatini M, Melchiorre C. J Med Chem. 2008; 51:347–372. [PubMed: 18181565]
13. Errington AC, Stohr T, Lees G. Curr Top Med Chem. 2005; 5:15–30. [PubMed: 15638775]
14. McNamara, JO. Goodman's & Gilman's The Pharmacological Basis of Therapeutics. 11. Brunton, LL.; Lazo, JS.; Parker, KL., editors. Vol. Chapter 19. McGraw-Hill; New York: 2006. p. 501-525.
15. Park KD, Morieux P, Salomé C, Cotten SW, Reamtong O, Eyers C, Gaskell SJ, Stables JP, Liu R, Kohn H. J Med Chem. 2009; 52:6897–6911. [PubMed: 19795888]
16. Park KD, Stables JP, Liu R, Kohn H. Org Biomol Chem. 2010; 8:2803–2813. [PubMed: 20405068]
17. Staub I, Sieber SA. J Am Chem Soc. 2009; 131:6271–6276. [PubMed: 19354235]
18. Hoffstrom BG, Kaplan A, Letso R, Schmid RS, Turmel GJ, Lo DC, Stockwell BR. Nat Chem Biol. 2010; 6:900–906. [PubMed: 21079601]
19. Peddibhotla S, Dang Y, Liu JO, Romo D. J Am Chem Soc. 2007; 129:12222–12231. [PubMed: 17880073]
20. Li Y-M, et al. Nature. 2000; 405:689–694. [PubMed: 10864326]
21. Ballell L, van Scherpenzeel M, Buchalova K, Liskamp RMJ, Pieters RJ. Org Biomol Chem. 2006; 4:4387–4394. [PubMed: 17102885]
22. Frick W, Bauer-Schafer A, Bauer J, Girbig F, Corsiero D, Heuer H, Kramer W. Bioorg Med Chem. 2003; 11:1639–1642. [PubMed: 12659749]
23. Hosoya T, Hiramatsu T, Ikemoto T, Nakanishi M, Aoyama H, Hosoya A, Iwata T, Maruyama K, Endo M, Suzuki M. Org Biomol Chem. 2004; 2:637–641. [PubMed: 14985799]
24. Adam GC, Sorensen EJ, Cravatt BF. Mol Cell Proteomics. 2002; 1:828–835. [PubMed: 12438565]
25. MacKinnon AL, Garrison JL, Hegde RS, Taunton J. J Am Chem Soc. 2007; 129:14560–14561. [PubMed: 17983236]
26. Sletten EM, Bertozzi CR. Angew Chem Int Ed. 2009; 48:6974–6998.

NIH-PA Author Manuscript NIH-PA Author Manuscript NIH-PA Author Manuscript

27. Saxon E, Bertozzi CR. Science. 2000; 287:2007–2010. [PubMed: 10720325]
28. Ovaa H, van Swieten PF, Kessler BM, Leeuwenburgh MA, Fiebiger E, van den Nieuwendijk AM, Galardy PJ, van der Marel GA, Ploegh HL, Overkleeft HS. Angew Chem Int Ed. 2003; 42:3626–3629.
29. Choi D, Stables JP, Kohn H. J Med Chem. 1996; 39:1907–1916. [PubMed: 8627614]
30. Perucca E, Yasothan U, Clincke G, Kirkpatrick P. Nat Rev Drug Disc. 2008; 7:973–974.
31. Errington AC, Stoehr T, Heers C, Lees G. Mol Pharmacol. 2008; 73:157–169. [PubMed: 17940193]
32. Sheets PL, Heers C, Stoehr T, Cummins TR. J Pharmacol Exp Ther. 2008; 326:89–99. [PubMed: 18378801]
33. Beyreuther BK, Freitag J, Heers C, Krebsfänger N, Scharfenecker U, Stöhr T. CNS Drug Rev. 2007; 13:21–42. [PubMed: 17461888]
34. Freitag JM, Beyreuther B, Heers C, Stoehr T. Epilepsia. 2007; 48(S6):320.
35. Temperini C, Innocenti A, Scozzafava A, Parkkila S, Supuran CT. J Med Chem. 2010; 53:850–854. [PubMed: 20028100]
36. de Costa BR, Lewin AH, Rice KC, Skolnick P, Schoenheimer JA. J Med Chem. 1991; 34:1531–1538. [PubMed: 2033577]
37. Rostovtsev VV, Green LG, Fokin VV, Sharpless KB. Angew Chem Int Ed. 2002; 41:2596–2599.
38. Tornoe CW, Christensen C, Meldal M. J Org Chem. 2002; 67:3057–3064. [PubMed: 11975567]
39. Speers AE, Cravatt BF. Chem Biol. 2004; 11:535–546. [PubMed: 15123248]
40. Levy, RH.; Mattson, R.; Meldrum, B. Antiepileptic Drugs. 4. Raven Press; New York: 1995. p. 99-110.
41. Ariëns EJ. Med Res Rev. 1986; 6:451–466. [PubMed: 3534485]
42. Wang Y, Park KD, Salome C, Wilson SM, Stables JP, Liu R, Khanna R, Kohn H. ACS Chem Neurosci. 2011; 2:90–106. [PubMed: 21532923]
43. LeTiran A, Stables JP, Kohn H. J Med Chem. 2002; 45:4762–4773. [PubMed: 12361404]
44. Liu D, Bienkowska J, Petosa C, Collier RJ, Fu H, Liddington R. Nature. 1995; 376:191–194. [PubMed: 7603574]
45. Petosa C, Masters SC, Bankston LA, Pohl J, Wang B, Fu H, Liddington RC. J Biol Chem. 1998; 273:16305–16310. [PubMed: 9632691]
46. Xiao B, Smerdon SJ, Jones DH, Dodson GG, Soneji Y, Aitken A, Gamblin SJ. Nature. 1995; 376:188–191. [PubMed: 7603573]
47. Obsil T, Ghirlando R, Klein DC, Ganguly S, Dyda F. Cell. 2001; 105:257–267. [PubMed: 11336675]
48. Fu H, Subramanian RR, Masters SC. Annu Rev Pharmacol Toxicol. 2000; 40:617–647. [PubMed: 10836149]
49. Watts RWE. J Clin Path Suppl. 1974; 8:48–63.
50. Long JZ, Li W, Booker L, Burston JJ, Kinsey SG, Schlosburg JE, Pavon FJ, Serrano AM, Selley DE, Parsons LH, Lichtman AH, Cravatt BF. Nat Chem Biol. 2009; 5:37–44. [PubMed: 19029917]
51. Stoehr T, Kupferberg HJ, Stables JP, Choi D, Harris RH, Kohn H, Walton N, White HS. Epil Res. 2007; 74:147–154.
52. Berg D, Holzmann C, Riess O. Nat Rev Neurosci. 2003; 4:752–762. [PubMed: 12951567]
53. Bridges D, Moorhead GBG. Sci STKE. 2005; 2005:re10. [PubMed: 16091624]
54. Wang H, Zhang L, Liddington R, Fu H. J Biol Chem. 1998; 273:16297–16304. [PubMed: 9632690]
55. Verazquez-Campoy, A.; Leavitt, SA.; Freire, E. Methods in Molecular Biology. In: Fu, H., editor. Protein-Protein Interactions: Methods and Protocols. Vol. 261. Humana Press; Totowa: 2004. p. 35-54.Chapter 3
56. Kovacs Z, Kekesi KA, Bobest M, Torok T, Szilagyi N, Szikra T, Szepesi Z, Nyilas R, Dobolyi A, Palkovits M, Juhasz G. J Neurosci Meth. 2005; 148:88–93.
57. Kekesi KA, Kovacs Z, Szilagyi N, Bobest M, Szikra T, Dobolyi A, Juhasz G, Palkovits M. Cell Mol Neurobiol. 2006; 26:833–844. [PubMed: 16897364]

NIH-PA Author Manuscript

NIH-PA Author Manuscript

NIH-PA Author Manuscript

58. Kovacs Z, Dobolyi A, Juhasz G, Kekesi KA. Neurochem Res. 2010; 35:452–464. [PubMed: 19856099]

59. Stover JF, Lowitzsch K, Kempski OS. Neurosci Lett. 1997; 238:25–28. [PubMed: 9464646]

60. Wishart DS, Lewis MJ, Morrissey JA, Flegel MD, Jeroncic K, Xiong Y, Cheng D, Eisner R, Gautam B, Tzur D, Sawhney S, Bamforth F, Greiner R, Li L. J Chromatogr B. 2008; 871:164–173.

61. Wiseman T, Williston S, Brandts JF, Lin L-N. Anal Biochem. 1989; 179:131–137. [PubMed: 2757186]

62. Allouis M, Le Bouffant F, Wilders R, Péroz D, Schott JJ, Noireaud J, Le Marec H, Mérot J, Escande D, Baró I. Circ Res. 2006; 98:1538–1546. [PubMed: 16728661]

63. Suginta W, Karoulias N, Aitken A, Ashley RH. Biochem J. 2001; 359:55–64. [PubMed: 11563969]

64. Li Y, Wu Y, Zhou Y. Neuron. 2006; 51:755–771. [PubMed: 16982421]

65. Wolff, C.; Carrington, B.; Van der Perren, C.; Vandendriessche, A.; Famelart, M.; Varrin-Doyer, M.; Gillard, M.; Foerch, P.; Rogemond, V.; Honnorat, J.; Lawson, A.; Miller, K. Abstracts of papers. 64th Annual Meeting of the American Epilepsy Society; San Antonio, TX. Dec 3–10, 2010; West Hartford, CT: American Epilepsy Society; 2010. p. Abstract 1.247

NIH-PA Author Manuscript

NIH-PA Author Manuscript

NIH-PA Author Manuscript

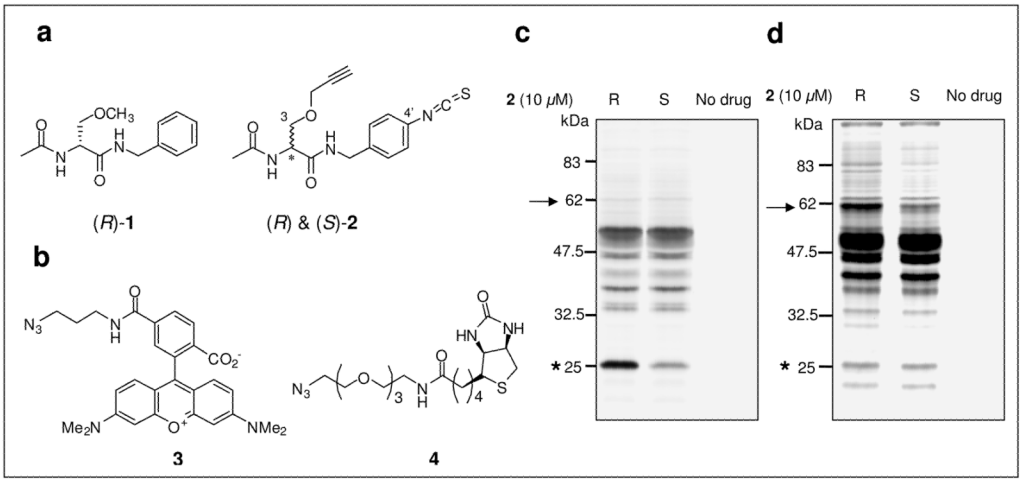

Figure 1.

Structures and proteome reactivity profiles. (a) Structures of lacosamide ((*R*)-**1**) and lacosamide AB&CR agent ((*R*)-&(*S*)-**2**). (b) Structures of rhodamine-azide (**3**) and biotin-azide (**4**) reporter probes. (c) Proteome reactivity profiles of lacosamide AB&CR **2** using the mouse brain soluble lysate. An asterisk marks selectively labeled protein by (*R*)-**2**. (d) Proteome reactivity profiles of lacosamide AB&CR **2** using the lysate precleared through a Nap-10 column. An arrow marks selectively labeled protein by (*R*)-**2**. All labeled proteins were detected by in-gel fluorescence scanning after Cu(I)-mediated cycloaddition to a rhodamine probe **3**. All proteins in lysate were visualized by Coomassie blue staining after in-gel fluorescence scanning. All images are shown in gray scale.

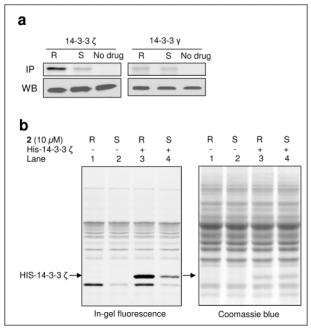

Figure 2.

Verification of 14-3-3 ζ. (a) Isoform-specificity of the adduction of 14-3-3 proteins by (*R*)-**2**. Anti-14-3-3 ζ and anti-14-3-3 γ antibodies were added to labeling/click reactions, immunoprecipitated (IP) and then analyzed by in-gel fluorescence scanning. Total amounts of both 14-3-3 ζ and 14-3-3 γ proteins were detected by western blot (WB) analysis. (b) In vitro labeling of mouse soluble lysate containing His-tagged 14-3-3 ζ with (*R*)-**2** and (*S*)-**2**. An arrow shows His-tagged 14-3-3 ζ protein. All proteins in lysate were visualized by Coomassie blue staining after in-gel fluorescence scanning. All images are shown in gray scale.

NIH-PA Author Manuscript NIH-PA Author Manuscript NIH-PA Author Manuscript

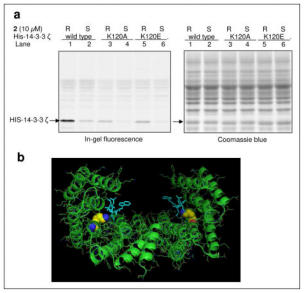

Figure 3.

Modification site of 14-3-3 ζ. (a) In vitro labeling of mouse soluble lysate containing K120-mutated, His-tagged 14-3-3 ζ proteins with (*R*)-**2** and (*S*)-**2**. His-tagged 14-3-3 ζ protein was marked with an arrow. All proteins in lysate were visualized by Coomassie blue staining after in-gel fluorescence scanning. All images are shown in gray scale. (b) The K120 residue projected as atom spheres lies adjacent to a key protein binding pocket in 14-3-3 ζ. R-18 peptide (cyan color) bound to the conserved amphipathic groove of 14-3-3 ζ. R-18 is an established, unphosphorylated peptide that binds tightly to 14-3-3 ζ (K_d= ~80 nM)[45] (PDB ID: 1A38).

NIH-PA Author Manuscript NIH-PA Author Manuscript NIH-PA Author Manuscript

NIH-PA Author Manuscript

NIH-PA Author Manuscript

NIH-PA Author Manuscript

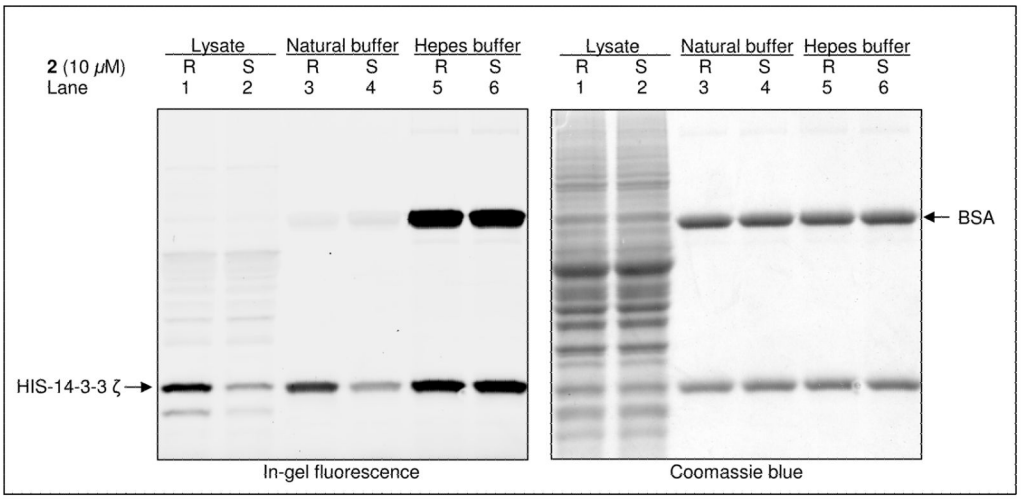

Figure 4.

(*R*)-**2** Selective modification of 14-3-3 ζ in the natural buffer. The mouse brain soluble lysate was passed through a Centricon 3K membrane filter, and the filtrate (natural buffer) was collected. His-tagged 14-3-3 ζ was added to the lysate, natural buffer and HEPES buffer (50 mM) and labeled with (*R*)-**2** and (*S*)-**2**. BSA served as a control protein in the natural and HEPES buffer (50 mM) experiments. All proteins were visualized by Coomassie blue staining after in-gel fluorescence scanning. All images are shown in gray scale.

NIH-PA Author Manuscript

NIH-PA Author Manuscript

NIH-PA Author Manuscript

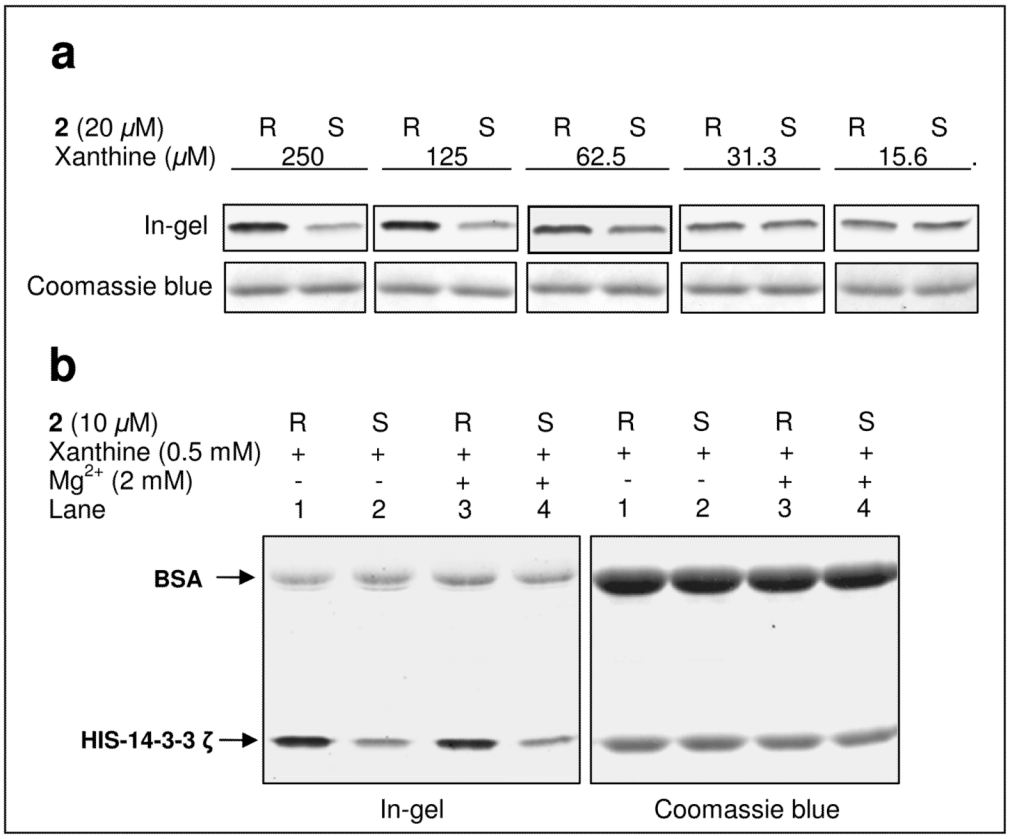

Figure 5.

Evaluation of the effect of xanthine on the adduction reaction. (a) Concentration-dependent effects of xanthine on (*R*)-**2** selective modification of His-tagged 14-3-3 ζ using HEPES buffer (50 mM). (b) (*R*)-**2** selective modification of His-tagged 14-3-3 ζ with/without divalent metal ion using HEPES buffer (50 mM). BSA was served as a control protein. Both proteins were visualized by Coomassie blue staining after in-gel fluorescence scanning. All images are shown in gray scale.

NIH-PA Author Manuscript

NIH-PA Author Manuscript

NIH-PA Author Manuscript

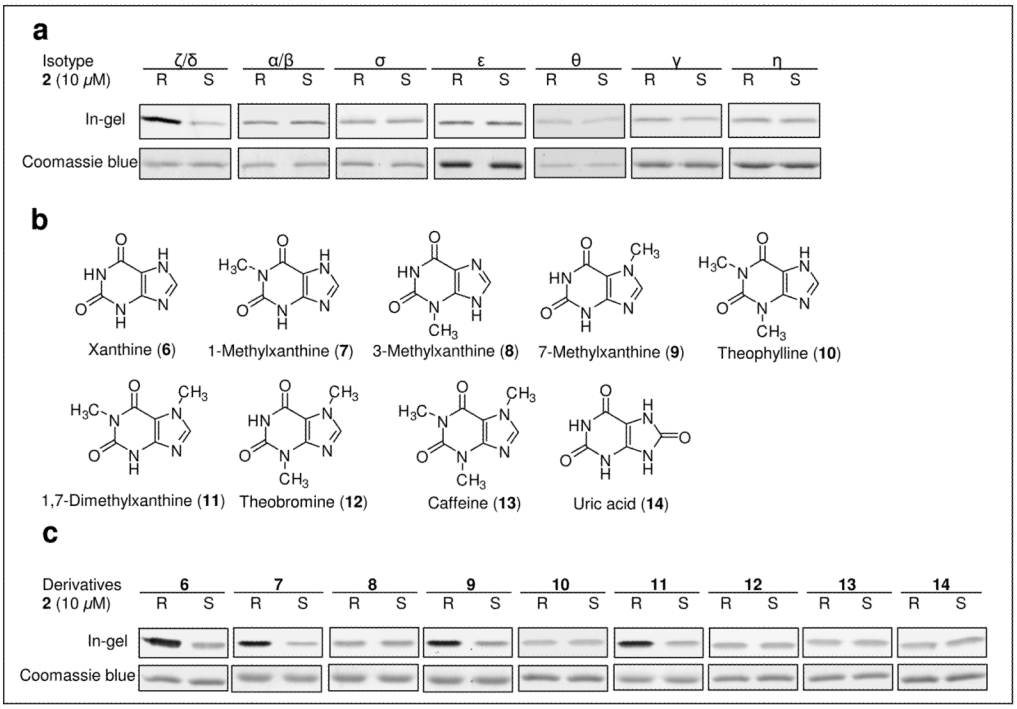

Figure 6.

Studies using 14-3-3 isoforms and xanthine derivatives. (a) In vitro labeling of seven 14-3-3 isoforms with (*R*)-**2** and (*S*)-**2** in the natural buffer. (b) Structures of xanthine derivatives. (c) Effects of xanthine derivatives on (*R*)-**2** selective modification of His-tagged 14-3-3 ζ using HEPES buffer (50 mM). 14-3-3 proteins were visualized by Coomassie blue staining after in-gel fluorescence scanning. All images are shown in gray scale.

NIH-PA Author Manuscript

NIH-PA Author Manuscript

NIH-PA Author Manuscript

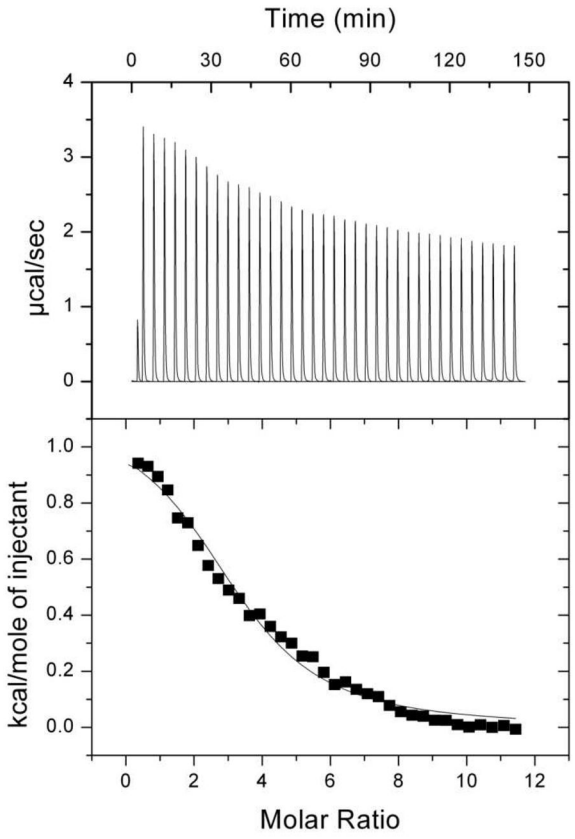

Figure 7.

Binding of 1,7-dimethylxanthine to His-tagged 14-3-3 ζ. (a) Calorimetric titration profile of aliquots of 10 mM 1,7-dimethylxanthine added to 0.2 mM His-tagged 14-3-3 ζ in 50 mM phosphate buffer, pH 7.6. (b) Sigmoidal plot of normalized titration isotherm. The solid line represents the best fitting curve calculated from one type of binding site model.

NIH-PA Author Manuscript

NIH-PA Author Manuscript

NIH-PA Author Manuscript

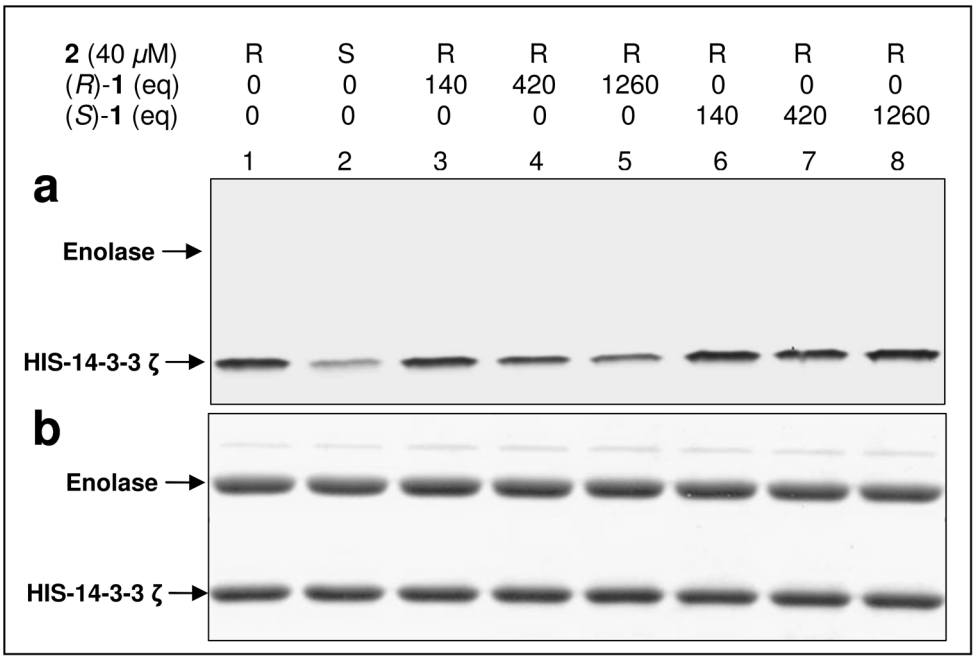

Figure 8.

Competition experiments using (*R*)-**2** with either excess (*R*)-**1** or (*S*)-**1** in the HEPES buffer (50 mM) including 0.5 mM of 1,7-dimethylxanthine. (a) His-tagged 14-3-3 ζ was detected by in-gel fluorescence scanning after adduction with (*R*)-**2** in the presence of excess **1** (room temperature, 2 min) followed by Cu(I)-mediated cycloaddition with **3**. Enolase served as a control protein. (b) Both proteins were visualized by Coomassie blue staining after in-gel fluorescence scanning. All images are shown in gray scale.